

A Fuzzy Logic Controller for IPMSG used in Wind Energy Conversion System

Ahmadreza Shafiei¹, Behzad Mirzaeian Dehkordi², Shahrokh Farhangi³ and Arash Kiyoumars⁴

¹ Ph.D. candidate, Department of Electrical Engineering, University of Isfahan, Isfahan, Iran
ahmad.shafiei@eng.ui.ac.ir

² Associate professor, Department of Electrical Engineering, University of Isfahan, Isfahan, Iran
mirzaeian@eng.ui.ac.ir

³ Professor, School of Electrical and Computer Engineering, University of Tehran, Tehran, Iran
Farhangi@ut.ac.ir

⁴ Associate professor, Department of Electrical Engineering, University of Isfahan, Isfahan, Iran
kiyoumars@eng.ui.ac.ir

Abstract :

In this paper a fuzzy logic based approach is presented for control of small-scale Wind Energy Conversion System (WECS) over wide operating range. The considered WECS is equipped with fixed-pitch blades and an Interior PM Synchronous Generator connected to a full-scale PWM rectifier. The proposed control strategy aims to track maximum power point at underrated wind speeds and harvest rated power of generator at overrated wind speeds. The space vector modulation-based direct torque control method is used to track the electrical torque and flux references. The reference of electrical torque is provided through a Fuzzy Logic Controller (FLC) achieving the maximum power point tracking. On the other hand, the reference flux magnitude is provided through a comprehensive strategy guarantying the machine operation over nominal rotational speed, limitation of the generated reference torque and copper-loss minimization. These are formulated as a *nonlinear optimization problem* which is solved numerically offline using the well-known sequential quadratic programming method. It should be noted that, the fuzzy rules are designed in such a way that not only result fast and accurate tracking performance at underrated wind speeds but also avoids irrational growth in reference electrical torque when the reference torque is limited by reference flux providing strategy. The proposed control strategy is verified by applying the strategy to a commercial 10 kW wind turbine simulated in MATLAB/Simulink.

Keywords: Direct-drive PMSG, Fuzzy Logic Control, SVM-DTFC, Wind Energy Conversion System.

Nomenclature

WECS	Wind energy conversion system
PMSM	Permanent magnet machine
PMSG	Permanent magnet synchronous generator
IPMSG	Interior PMSG
SMPMSG	Surface Mounted PMSG
FOC	Field oriented control
DTC	Direct torque control
SVM-DTC	Space vector modulation based direct torque control
FLC	Fuzzy logic controller
SQP	Sequential quadratic programming
MPPT	Maximum power point tracking
MPP	Maximum power point
MTPA	Maximum torque per ampere
OTSR	Optimal Tip Speed Ratio

1. Introduction¹

Nowadays, increasing demands of energy, reducing fossil fuel resources, and their rising cost besides environmental issues have made renewable energy sources more attractive than before. Over 318 GW installed capacity of wind power generation systems in the range of few hundred watts to several megawatts indicates that wind energy is financially effective, reachable, and technologically advanced [1].

Small scale WECSs, ranging from 0.02 kW to 100 kW, with Off- or On-grid installation are considered as renewable distributed generations which can be utilized by domestic or commercial

² Submission date: 24 , 10 , 2015

Acceptance date: 16 , 07 , 2016

Corresponding author: Behzad Mirzaeian Dehkordi,

customers [2]. A WECS equipped with direct-drive PMSG and full scale voltage source converter is a promising variable speed WECS which has been studied widely in recent years [3, 4]. This configuration has been adopted predominantly in new small scale WECSs. Some advantages of this structure are as follows:

- Absorbing maximum achievable aerodynamic power due to its variable speed structure.
- Mechanical stress, loss, and failure reduction regarded to gearbox elimination.
- Size, weight, and power loss reduction of WECS due to using PM generator.

In order to extract maximum aerodynamic power, a fast and accurate speed tracking technique should be applied to the generator control unit. A review on reported works shows that the typical adopted method for PMSG control is FOC. In the last two decades DTC method has been developed and improved to control PMSM. Although the DTC has simpler structure, faster response, and more robust against parameter uncertainties, suffers from higher torque and flux ripples and variable switching frequency [5]. SVM-DTC is a proposed method for motor control with smoother torque and flux [6, 7]. Although, in this approach direct control of torque and flux are associated with a reference frame transformation, the fast response and parameter independency of DTC is retained [7].

Typically, control of WECS at overrated wind speeds, named stalling mode, is done by reduction of rotor speed while maintaining the power to the rated value. In this mode the generator would try to overcome turbine mechanical torque by increasing electrical torque. This would yield more fluctuations in rotor speed and the harvested power of generator [8]. Rotation of the turbine and generator at speeds higher than the nominal speed is an alternative approach for WECS control at over rated wind speeds which could maintain the power to the rated value. Compared to latter, the former approach causes overdesign issues, that is to say, requiring a generator with higher rated power than that of its associated turbine [8] (cf. section 2.1 for more details).

Motivated by the above arguments, we use the method in which the rotational speed is increased to maintain the rated power. The flux weakening is the only method by which the operation of the permanent magnet synchronous machine over nominal rotational speed is possible. While the strategy has been widely

used for motor operation, a few attempts have been made towards PMSG used in renewable energy systems including wind [8-10] and marine current turbines [11], with which this paper is primarily concerned. Normally, the flux weakening affects the method by which the references of currents (in FOC method [8, 10, 11]) or flux magnitude (in DTC methods [9]) are generated. Thus, contrary to methods proposed by [12-15], a separate controller is not required to control WECS at overrated wind speeds.

In this paper, a novel overall power control strategy is designed in such a way that the WECS efficiently operates for both underrated and overrated wind speeds. The generator control is based on SVM-DTC. Thus, this paper contributes to the literature by introducing new strategies providing references for electrical torque and flux magnitude. At underrated wind speeds, the reference electrical torque is generated in such a way that MPPT is guaranteed. To this end, a regulator is used to bring the measured rotational speed to its optimal value. The optimal rotational speed is calculated based on OTSR [16, 17] (cf. section 2.1 for more details).

The WECS is a nonlinear and uncertain plant which its operating point varies time to time due to fast variations of wind speed. The conventional PI controller is a commonly used controller with simple structure and effective performance. However, it does not present the same performance in dealing with multi-operating point nonlinear systems. Instead, a FLC could be confronted with such plant successfully. The FLC takes advantage of heuristics and expert knowledge of the process being controlled making it adaptive in nature, insensitive to parameter variations, robust to uncertainties and mathematical model-free. These offer superiority of FLC over conventional methods. Thus, in this work, a FLC is adopted to replace the conventional PI controller for the sake of reference generation for electrical torque. At overrated wind speed, the FLC still attempts to provide the MPPT regardless of the generated power, which may damage the machine. To tackle the difficulty, a torque limiting strategy is considered in reference flux providing strategy. However, this causes irrational growth in the output of FLC during torque limitation interval. Therefore, an extra fuzzy input together with appropriate rules are considered to avoid mentioned phenomenon. This modification not only makes proposed FLC different from FLC used in [14, 18-20], but also enforces the

response of FLC.

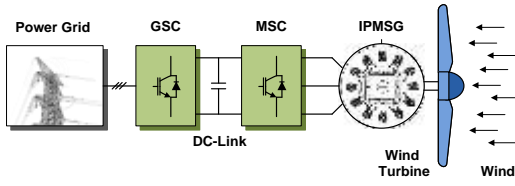


Fig (1): Structure of studied WECS composed of direct-drive IPMSG, fully controlled PWM rectifier and grid-tie inverter.

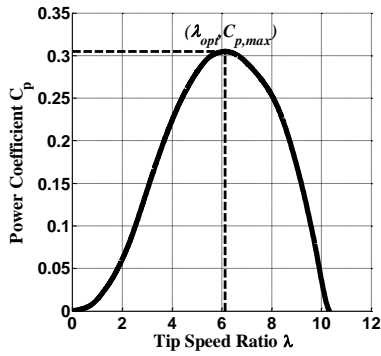


Fig (2): $C_p - \lambda$ curve of studied WECS

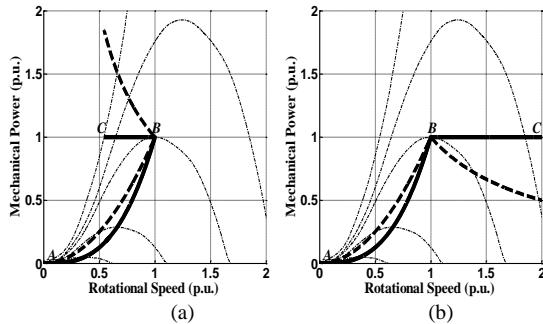


Fig (3): Aerodynamic characteristics of wind turbine. (a) Mechanical power (solid) and torque (dashed) of turbine as function of rotational speed via soft-stalling method (b) Mechanical power (solid) and torque (dashed) of turbine as function of rotational speed via flux-weakening method.

As mentioned earlier, the reference of flux magnitude should be provided precisely to allow machine operation over nominal rotational speed. On the other hand, the flux magnitude affects the copper losses of windings. Thus, the flux magnitude is determined using approximated polynomial [9] and look-up table [21] with the aim of copper loss minimization. In this paper, a new approach is proposed to provide optimal reference flux through designing an optimization problem. The flux weakening and copper loss minimization are simultaneously

achieved by numerically solving the optimization problem. In particular, SQP method is used to solve the problem offline and the results are stored in a look-up table for fast online use. Based on the reference electrical torque and the measured rotational speed, the optimal flux magnitude is obtained from the lookup table. To provide the desired voltage vector, the references of electrical torque and flux magnitude are applied to SVM-DTC. To the best of our knowledge, such an overall control strategy has not been proposed in the literature yet. Finally, we illustrate the effectiveness of our overall power control strategy by applying a commercial 10 kW wind turbine simulated in MATLAB/Simulink.

The rest of this paper is arranged as follows: section II briefly reviews the mathematical modeling of wind turbine and generator. The details of the proposed controller are presented in section III. Simulation results and related discussions are given in section IV and finally the paper is concluded in section V.

2. Structure of the studied wind energy conversion system

An IPMSG-based direct-drive WECS consists of a generator, a machine side converter, DC-link and grid side converter. In spite of low cost, a diode rectifier suffers from inherent uncontrollability and significant stator current harmonics [4]; thus a PWM rectifier with full controllability is used in this work.

This study just tries to focus on controlling machine side converter. Thus, the control of grid side generator is neglected and it is assumed that DC-link voltage is controlled at a predefined value using grid side converter. The structure of the studied WECS is illustrated in Fig. 1.

2.1. Aerodynamics of wind turbine

The precise modeling of the wind turbine aerodynamics is highly difficult to determine. In most practical cases, the aerodynamic power of the turbine is given by [22]

$$P = 0.5\pi\rho C_p(\lambda, \beta) R_t^2 v_w^3 \quad (1)$$

where R_t is turbine radius, V_w is wind speed, ρ is air density, β is pitch angle, C_p is power coefficient. λ is tip speed ratio which is defined by:

$$\lambda = \frac{\omega_r R_t}{v_w} \quad (2)$$

where ω_r is the angular speed of rotor.

Normally, the small scale WECS are fixed pitch; therefore, the power coefficient is only a function of tip speed ratio. In this paper a 10kW wind turbine with $C_p - \lambda$ curve illustrated in fig. 2 is studied.

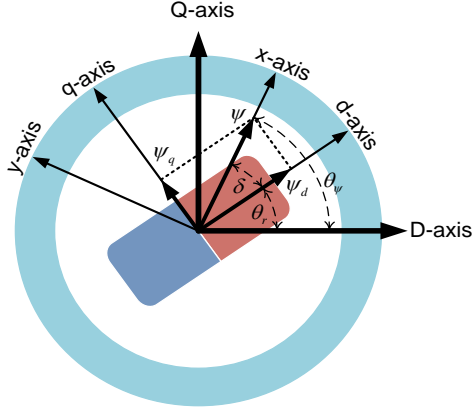


Fig (4): Different coordinate reference frames used for PMSM modeling; (DQ coordinate) two-axis stationary reference frame, (dq coordinate) rotor flux reference frame, (xy coordinate) stator flux reference frame.

According to (1), the maximum aerodynamic power for a specific wind speed is achieved at the peak of $C_p - \lambda$ characteristic. As depicted in Fig. 2, the peak point corresponds to the pair $(\lambda_{opt}, C_{p,max})$. Substituting λ_{opt} in (2) provides the rotor speed corresponding with the maximum achievable aerodynamic power at each wind speed, that is

$$\omega_{r,opt} = \frac{\lambda_{opt} v_w}{R_t} \quad (3)$$

Based on (3), a MPPT method known as OTSR is developed which uses the measured wind speed to determine reference of rotational speed. As the wind speed increases, the rotational speed should be increased to keep the MPPT (c.f. the path AB in Figs. 3a and 3b). When the generator power reaches its rated limit at point B, the captured power should be limited to the rated value. Towards this end, there are two approaches [8, 12]:

- reduction of the rotational speed while maintaining the power to the rated value (c.f. the path BC in Fig. 3a),
- Increase of the rotational speed while maintaining the power to the rated value (c.f. the path BC in Fig. 3b).

The former is known as soft-stalling

approach. The latter is long with flux-weakening operation, so we name it flux-weakening approach. According to the dashed lines in Figs. 3a and 3b, the generator controlled with soft-stalling approach must be capable of providing higher torques than that with flux-weakening, which imposes higher cost and weight to WECS. The flux-weakening approach is indeed applicable provided that some appropriate control method is carried out. Moreover, the WECS should be protected against severe wind speeds. In practice, the WECS is equipped with an over-speed mechanism designed to protect the turbine's mechanical components from damage during high winds. This mechanism is referred to as an auto-furling mechanism and functions by positioning, or yawing the turbine rotor away from the incoming wind (cf. [23] and [24] for more details).

2.2. Direct-Drive IPMSG

Gearbox and exciting system elimination from the direct-drive IPMSG based WECS, has made it economical and preferable for small scale application. In comparison with a gearbox mounted generator, a direct-drive generator has higher number of poles and consequently has bigger diameter. In addition, the electromagnetic torque of a direct-drive generator should be higher.

Regarding to reluctance torque, the IPMSG benefits from higher torque and power; thus IPMSG is used instead of conventional SMPMSG. The reduced-order model of IPMSG in the stator flux reference frame which is aligned with stator flux vector is described by (cf. Fig.4 for more details):

$$v_d^{w_s} = R i_d^{w_s} + \frac{d\psi_s}{dt} \quad (4)$$

$$v_q^{w_s} = R i_q^{w_s} + \omega_{w_s} \psi_s \quad (5)$$

where $v_d^{w_s}$, $v_q^{w_s}$ are the stator voltage components, respectively, $i_d^{w_s}$, $i_q^{w_s}$ are the stator current components, respectively, ω_{w_s} is the electrical angular velocity of stator flux vector and R is the stator resistance. The produced torque of machine is defined by:

$$T_e = \frac{3p}{4} \psi_s i_q^{w_s} \quad (6)$$

where p is the number of machine poles.

3. Structure of the Proposed

Controller

As mentioned earlier, a control scheme is required such that a MPPT is obtained when the wind speed lies below rated wind speed; on the other hand, the control scheme should confine the generator power to its rating value when the wind speed exceeds rated value. On the contrary to large scale turbines, the pitch control unit is eliminated in small scale turbine to reduce complexity and cost of system. Thus the generator control unit is the only unit contributing to implementation of the control scheme regardless of the wind speed value [12, 14, 25].

While the MPPT problem has been studied in depth [16, 26-28], a few works have been reported on development of an overall control strategy which is applicable over wide wind speed range [8, 10-15, 25, 29, 30].

When the wind speed lies below the rated wind speed, the controller should keep the MPPT by a fast response control method. On the other hand, the control scheme should confine the

generator power to its rated value by increasing the rotational speed beyond rated value when the wind speed exceeds the rated value. This approach is indeed applicable provided that some appropriate control method is carried out. The SVM-DTFC is a control method adopted in this work because of its fast response, decoupled control of torque and flux, and facilitated flux weakening operation over rated speed.

As depicted in Fig. 5, the reference of electrical torque is generated by a FLC aiming to track the MPP regardless of the generated power. This may result an operating point outside machine limitation which is unreachable or damageable for machine. To tackle the difficulty, an approach is designed determining the reference of flux magnitude based on machine constraints and restricting the reference electrical torque. Moreover, the copper loss minimization is augmented to this approach to improve the machine efficiency.

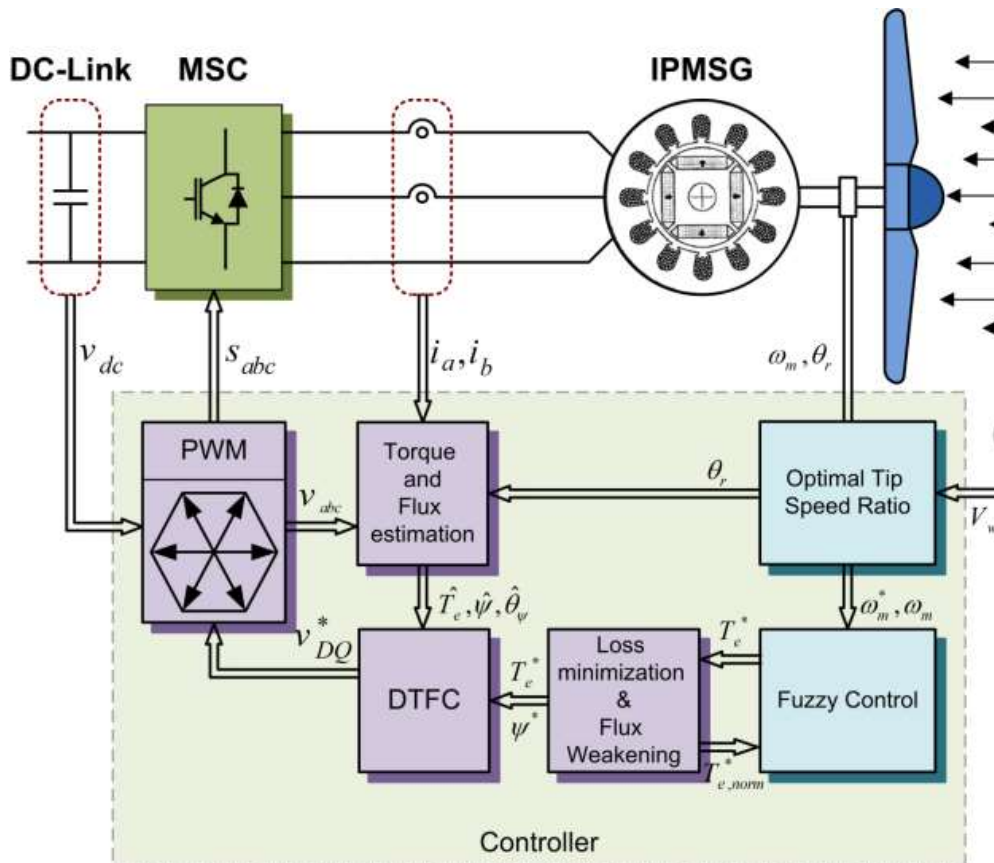


Fig (5): Structure of Proposed Controller.

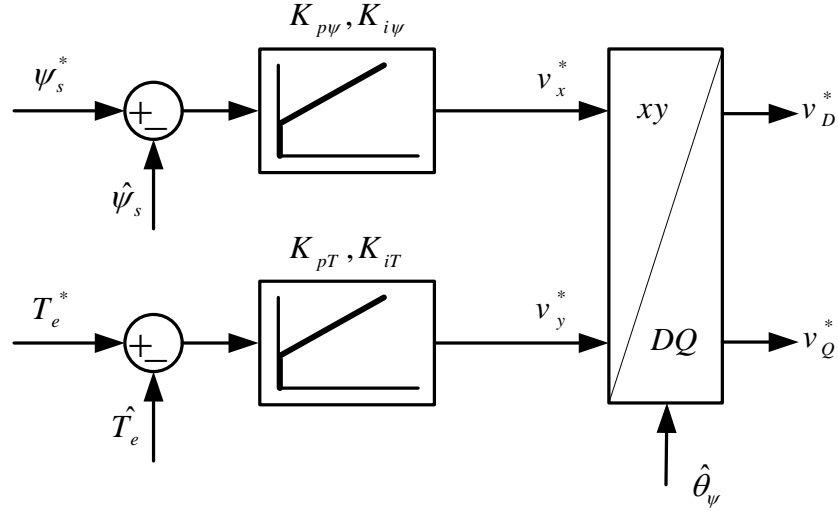


Fig (6): Torque and flux control loops inside DTFC block of fig. 5.

3.1. Principle of SVM-DTFC

The SVM-DTFC is based on machine voltage equations transformed to stator flux reference frame. According to (4), the d -axis component of voltage can be adopted to control the flux magnitude. On the other hand, based on (5) and (6), the electromagnetic torque of machine would be controlled using q -axis component of stator voltage, provided that $\omega_\psi \psi_s$ is cancelled via a feed-forward compensation term. Due to the faster dynamic of electrical system in comparison with mechanical system, the feed-forward term can be omitted [7, 21]. Therefore, two PI controllers are considered for reference voltage generation from flux and torque error as:

$$v_x^* = \left(K_{p\psi} + \frac{K_{i\psi}}{S} \right) (\psi_s^* - \psi_s) \quad (7)$$

$$v_y^* = \left(K_{pT} + \frac{K_{iT}}{S} \right) (T_e^* - T_e) \quad (8)$$

As illustrated in Fig. 6 the outputs of controllers are transferred to stationary reference frame based on the estimated flux angle $\hat{\theta}_\psi$ and utilized in SVM in order to generate switching pulses.

3.2. Reference Providing for Stator Flux

According to (6), there are infinitely many pairs of $(\psi_s, i_q^{\psi_s})$ yielding the desired electromagnetic torque. However, there is one pair which not only gives the desired electromagnetic torque, but also minimizes the copper loss (cf. Fig.7 intersections of the solid line with the dashed

line; e.g. points A and B). This is regarded as a criterion for reference flux selection causing improvement in the system efficiency. Moreover the current and voltage constraints of machine and converter should be taken into account for reference flux selection. Consideration of mentioned constraints ensures the operation of WECS over rated wind speed without extra control method. Based on above mentioned points, an approach is presented to select the references for flux magnitude in such a way that the copper loss is minimized, the desired electromagnetic torque is obtained and the voltage and current constraints are satisfied, simultaneously. These verbal arguments can be converted into the following mathematical problem.

$$\begin{aligned} & \min_{\psi_s, \delta} f(\psi_s, \delta) \\ & \text{subject to: } g(\psi_s, \delta) = 0, \end{aligned} \quad (9)$$

$$h_1(\psi_s, \delta) \leq 0,$$

$$h_2(\psi_s, \delta) \leq 0$$

where

$$f(\psi_s, \delta) = \frac{\psi_s^2}{2} \left(\frac{1}{L_q^2} + \frac{1}{L_d^2} \right) - \frac{\psi_s^2}{2} \left(\frac{1}{L_q^2} - \frac{1}{L_d^2} \right) \cos 2\delta - \frac{2\psi_s \psi_{pm}}{L_d^2} \cos \delta + \frac{\psi_{pm}^2}{L_d^2} \quad (10)$$

$$g(\psi_s, \delta) = \frac{\psi_s^2}{2} \left(\frac{1}{L_q} - \frac{1}{L_d} \right) \sin 2\delta + \frac{\psi_s \psi_{pm}}{L_d} \sin \delta - \frac{4T_e^*}{3p} \quad (11)$$

$$\begin{aligned} h_1(\psi_s, \delta) &= \frac{R_s^2 \psi_s^2}{2} \left(\frac{1}{L_q^2} + \frac{1}{L_d^2} \right) - \frac{R_s^2 \psi_s^2}{2} \left(\frac{1}{L_q^2} - \frac{1}{L_d^2} \right) \cos 2\delta \\ &+ a_\psi^2 \psi_s^2 - \frac{2R_s^2 \psi_s \psi_{pm}}{L_d^2} \cos \delta + \frac{R_s^2 \psi_{pm}^2}{L_d^2} + \frac{8}{3p} R_s a_\psi T_e^* \\ &- \bar{U}_{\max}^2 \end{aligned} \quad (12)$$

$$h_2(\psi_s, \delta) = f(\psi_s, \delta) - I_{\max}^2 \quad (13)$$

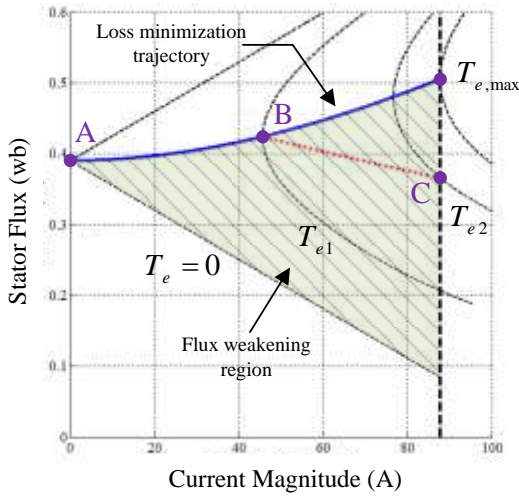


Fig (7): Calculated operating points for a given rotational speed above nominal value and a set of torque values (path ABC) in $\psi_s - I$ plane.

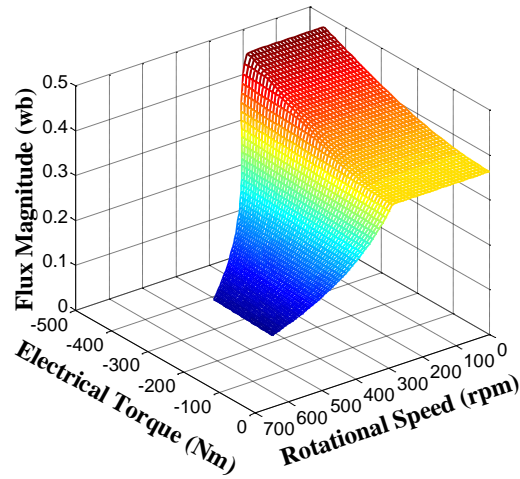


Fig (8): 3D plot of calculated flux magnitudes as function of rotational speed and electrical torque

where L_d and L_q are the d- and q-axis inductances, respectively; ψ_{pm} is the flux linkage generated by the permanent magnet; U_{\max} and I_{\max} are, respectively, the maximum values of voltage and current. The objective function $f(\dots)$ provides minimization of copper loss, due to the facts (10) is equal to $i_d^2 + i_q^2$ where i_d and i_q are the stator current components in synchronously rotating rotor reference frame

given by

$$i_d = \frac{\psi_s \cos \delta - \psi_{pm}}{L_d} \quad (14)$$

$$i_q = \frac{\psi_s \sin \delta}{L_q}. \quad (15)$$

The equality constraint $g(\dots)$ represents the torque equation. The inequalities $h_1(\dots)$ and $h_2(\dots)$ represent the voltage and current constraints, respectively.

Among the numerous solution methods for constrained nonlinear optimization problem, the Sequential Quadratic Programming (SQP) method is one of the most successful methods in terms of efficiency, accuracy and percentage of successful solutions over a large number of test problems [31]

In this paper, the SQP method is used to find individual optimal flux magnitude related to each pair of desired electromagnetic torque and rotational speed (T_e^*, ω_r) . To reduce online computation burden, the problem (9) is solved off-line. Particularly, the Matlab optimization toolbox is exploited to solve this problem. For this purpose, first, N samples of rotational speed equidistantly are picked and the vector of the maximum allowable torque associated with the speed samples is obtained. Then, a vector containing N samples of electromagnetic torque is obtained for each speed sample by equidistant sampling between zero and maximum allowable torque associated with the speed sample. Finally, the flux magnitudes are calculated for all $M \times N$ pairs of (T_e^*, ω_r) and stored in a look-up table. Figs. 8 shows 3D plots associated with this look-up table.

It should be noted that our method still works when the operating point resides out of machine limitation. In this case, a torque limiting procedure is activated and replaces the desired electromagnetic torque by the maximum allowable torque associated with its rotational speed. In this way, the operation of the WECS over rated wind speed is guaranteed.

3.3. Reference Providing for Electrical Torque

At underrated wind speeds, the reference electrical torque is generated in such a way that

MPPT is guaranteed. As mentioned earlier, the OTSR is a MPPT method which provides optimal rotational speed. Thus, a controller is required to stabilize the rotational speed at $\omega_{r,opt}$. Moreover, using (1), $T_m = P_m / \omega_r$ and optimal pair of $(\lambda_{opt}, C_{p,max})$ with some manipulations, optimal mechanical torque of turbine

$$T_{m,opt} = 0.5\pi\rho C_{p,max} R_r^5 \omega_r^2 / \lambda_{opt}^3 =: k_{opt} \omega_r^2 \quad (16)$$

is obtained introducing another approach based on OTSR. Inspired by (16), the MPPT is achieved by a controller regulating the mechanical torque at $T_{m,opt}$. This approach requires mechanical torque measurement instead of wind speed measurement, which is not conventional. In [9-11, 32,33] the dynamical behavior of the WECS is neglected and the $T_{m,opt}$ is utilized directly as the reference of electrical torque. As proven by simulations, this degrades the performance of MPPT. Therefore, we use a controller to regulate the rotational speed at $\omega_{r,opt}$.

3.4. FLC design for speed regulation

In this work, Fuzzy Logic Control (FLC) is adopted to replace the conventional PI controller for the sake of speed regulation. The FLC takes advantage of heuristics and expert knowledge of the process being controlled making it adaptive in nature, insensitive to parameter variations, robust to uncertainties and mathematical model-free. These offer superiority of FLC over conventional methods.

To achieve the speed regulation task, the reference electrical torque T_e^* is assigned to the output of the FLC. The scaled versions of the speed error e_ω and its difference Δe_ω as well as limited version of reference torque $T_{e,norm}^*$ are the actual inputs of fuzzy system. As illustrated in Fig. 9 the fuzzification of the inputs and output of the FLC is performed using uniformly distributed triangular and trapezoidal membership functions.

The fuzzy subset of e_ω , Δe_ω and T_e^* are divided into [NB,NM,NS,Z,PS,PM,PB] which stand for Negative Big, Negative Medium,

Negative Small, Zero, Positive Small, Positive Medium, and Positive Big, respectively. Also The fuzzy subset of $T_{e,norm}^*$ is divided into [Z,N,R] which stand for Zero, Normal and Rated torque, respectively.

Based on this fuzzy set, a fuzzy reasoning database with 49 rules is established for speed regulation within machine limitations which is listed in TABLE I. All rules are designed in such a way that results negative value for generative operation of machine. In addition, the rule base is designed to consider the following verbal expressions:

- IF the actual speed is lower than reference THEN a lower torque should be applied i.e. a positive change in output would occur.
- IF the actual speed is higher than reference THEN a higher torque should be applied i.e. a negative change in output would occur.
- IF the actual speed is equal to the reference THEN no additional torque should be applied i.e. the output should be zero.

At overrated wind speed, the FLC still attempts to provide the MPPT regardless of the generated power, which may damage the machine. To tackle the difficulty, a torque limiting strategy is considered in reference flux providing strategy. However, this causes irrational growth in the output of FLC during torque limitation interval. To avoid this situation, following verbal expressions is considered:

- IF the generated reference torque exceeds the machine ratings, no more negative change is acceptable,
- IF the generated reference torque is positive (motor operation), no more positive change is acceptable,

which are implemented using $T_{e,norm}^*$ input and rules given in TABLE II and TABLE III. It should be noted that, $T_{e,norm}^* := |T_{e,lim}^* / T_{max}(\omega_r)|$ is the normalized absolute value of limited T_e^* . The $T_{e,norm}^*$ is a value between 0 and 1. The zero value of $T_{e,norm}^*$ indicates that no power is delivered to grid, while a value equal to one indicates that the rated power is delivered.

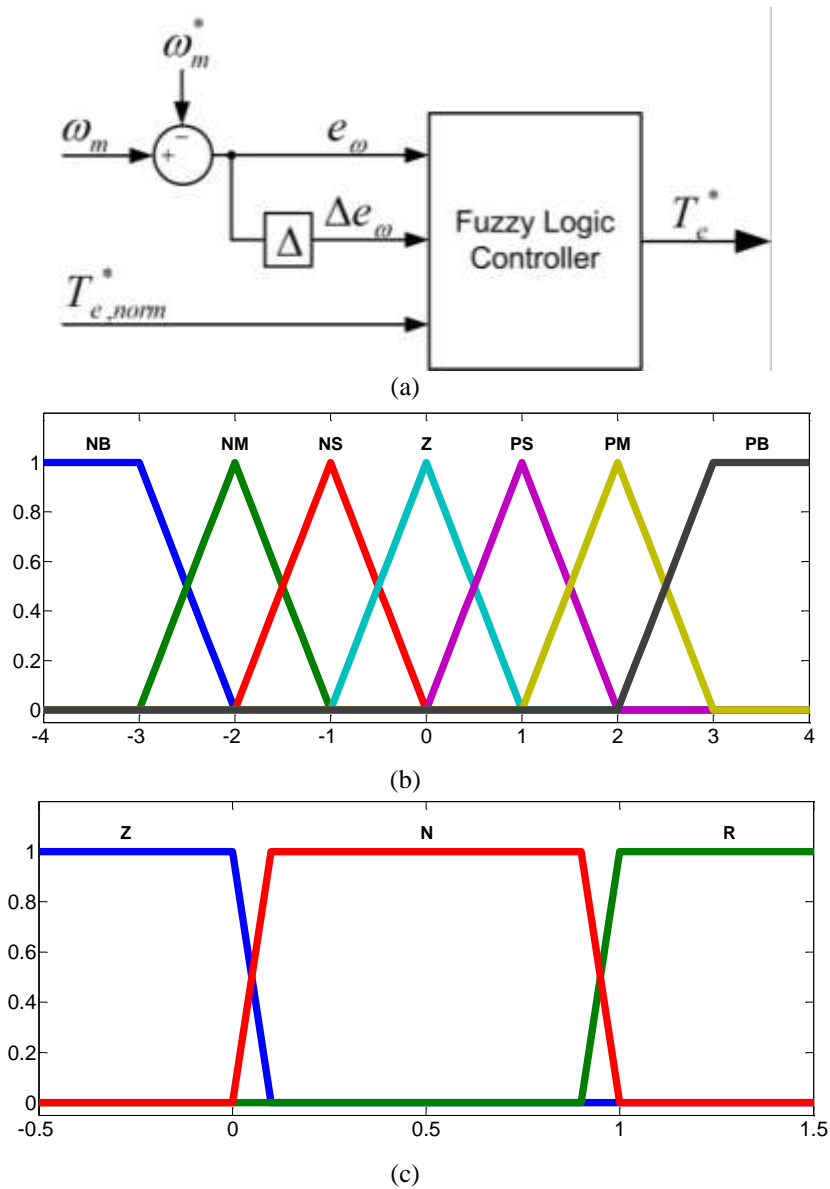


Fig (9): Proposed FLC. (a) input and outputs of FLC (b) membership functions of e_ω , Δe_ω and T_e^* (c) membership functions of $T_{e,norm}^*$.

Table (1): The Fuzzy Rule Set for Speed Control when $T_{e,norm}^* = N$

ΔT^*		Δe_ω						
		NB	NM	NS	Z	PS	PM	PB
e_ω	NB	PB	PB	PB	PM	PM	PM	PS
	NM	PB	PB	PM	PM	PM	Z	NB
	NS	PB	PM	PM	PM	PS	NS	NB
	Z	PB	PM	PS	Z	NS	NM	NB
	PS	PB	PS	NS	NM	NM	NM	NB
	PM	PB	Z	NM	NM	NM	NB	NB
	PB	NS	NM	NM	NM	NB	NB	NB

Table (2): The Fuzzy Rule Set for Speed Control when $T_{e,nom}^* = R$

ΔT^*		Δe_ω						
		NB	NM	NS	Z	PS	PM	PB
e_ω	NB	PB	PB	PB	PM	PM	PM	PS
	NM	PB	PB	PM	PM	PM	Z	Z
	NS	PB	PM	PM	PM	PS	Z	Z
	Z	PB	PM	PS	Z	Z	Z	Z
	PS	PB	PS	Z	Z	Z	Z	Z
	PM	PB	Z	Z	Z	Z	Z	Z
	PB	Z	Z	Z	Z	Z	Z	Z

Table (3): The Fuzzy Rule Set for Speed Control when $T_{e,nom}^* = Z$

ΔT^*		Δe_ω						
		NB	NM	NS	Z	PS	PM	PB
e_ω	NB	Z	Z	Z	Z	Z	Z	Z
	NM	Z	Z	Z	Z	Z	Z	NB
	NS	Z	Z	Z	Z	Z	NS	NB
	Z	Z	Z	Z	Z	NS	NM	NB
	PS	Z	Z	NS	NM	NM	NM	NB
	PM	Z	Z	NM	NM	NM	NB	NB
	PB	NS	NM	NM	NM	NB	NB	NB

4. Simulation results

To verify the effectiveness of proposed control structure, numerical simulations are done in MATLAB/ Simulink. In order to verify control performance on a real wind turbine, the parameters of simulated wind turbine are borrowed from a real turbine named Bergey Excel-S 10 kW [34]. The parameters of turbine are given in TABLE IV.

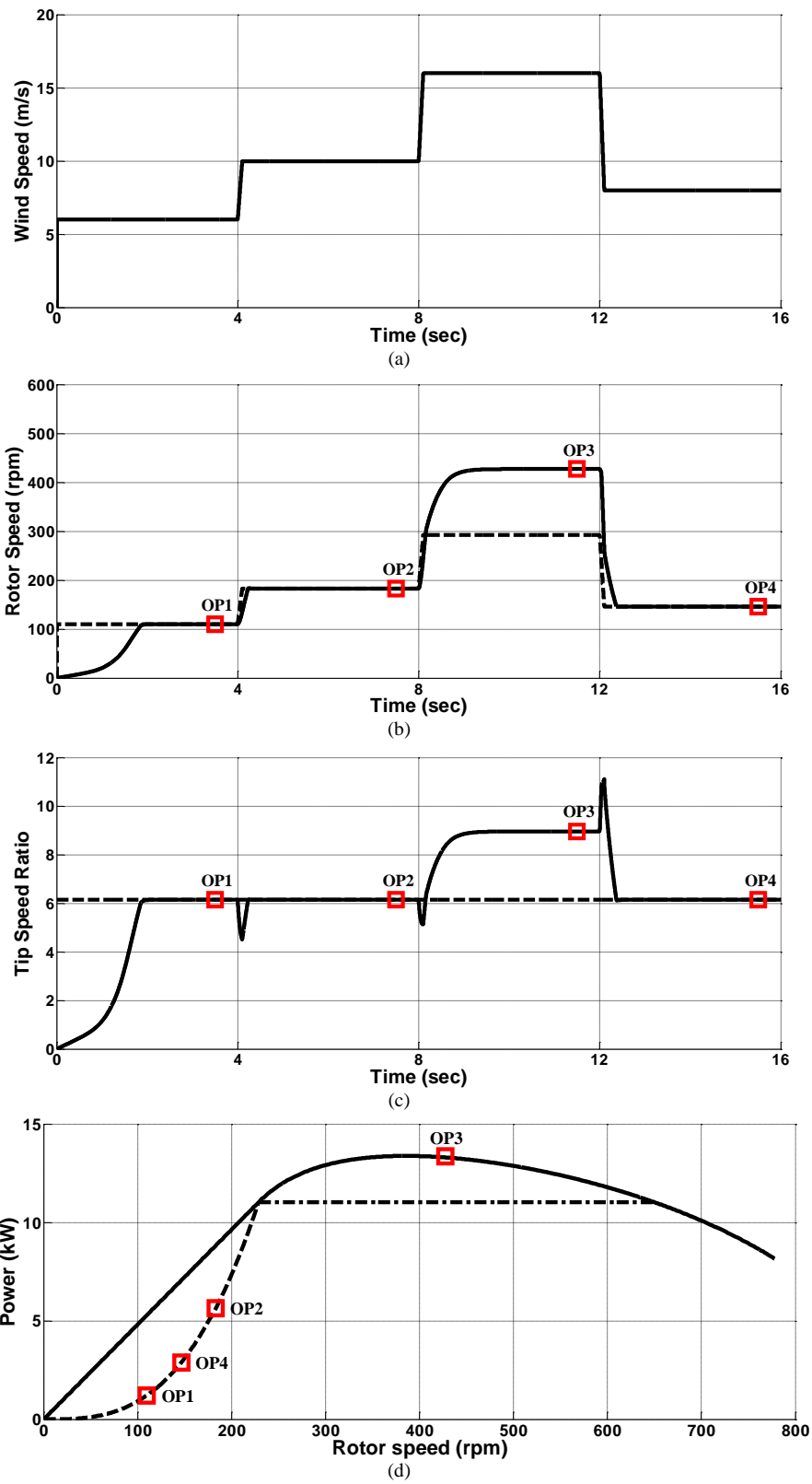
Table (4): Parameters of Wind Energy Conversion System

Parameters	value
Nominal DC Voltage	400 V
Nominal rotor Speed	229 r/min
Nominal Power of WECS	10 kW
Nominal Torque (T_N)	460 Nm
Number of poles (p)	42
Stator resistance (R)	0.25 Ω
Direct-axis inductance (L_d)	6.6 -mH
Quadrature-axis inductance (L_q)	11 mH
Permanent magnet flux (ψ_{pm})	0.3629 Vs
Rotor Radius	3.203 m
Number of Blades	3
Rated Wind Speed	12.5 m/s

Cut-in Wind Speed	3.1 m/s
Optimal Tip speed Ratio (λ_{max})	6.15
Maximum Power Coefficient ($C_{p,max}$)	0.3048
Total moment of inertia (J)	7.71 kgm ²

The DC-link voltage is 400 V which is sufficient for a grid-tie inverter producing a 220 V single phase ac voltage. The sampling period of control strategy is 100 μ s and the FLC is executed every 10 samples. These sampling rates are typical for practical applications. This allows SVM-DTC to track the last generated command effectively. The scaling gains of the FLC are set to $K_{e_\omega} = 10$, $K_{\Delta e_\omega} = 700$ and $K_{T_e^*} = 5$.

Since the actual wind speed varies time to time, the performance of control system in transient and steady-state operation is examined by step changes in wind speed. As depicted in Fig 10(a), a fast step changing wind profile with 3 step changes is applied to WECS and results are illustrated in Fig. 10. To clarify the accuracy of controller in steady state, 4 time instants sufficiently far from step time are selected and the operating points corresponding to them are marked on all curves.



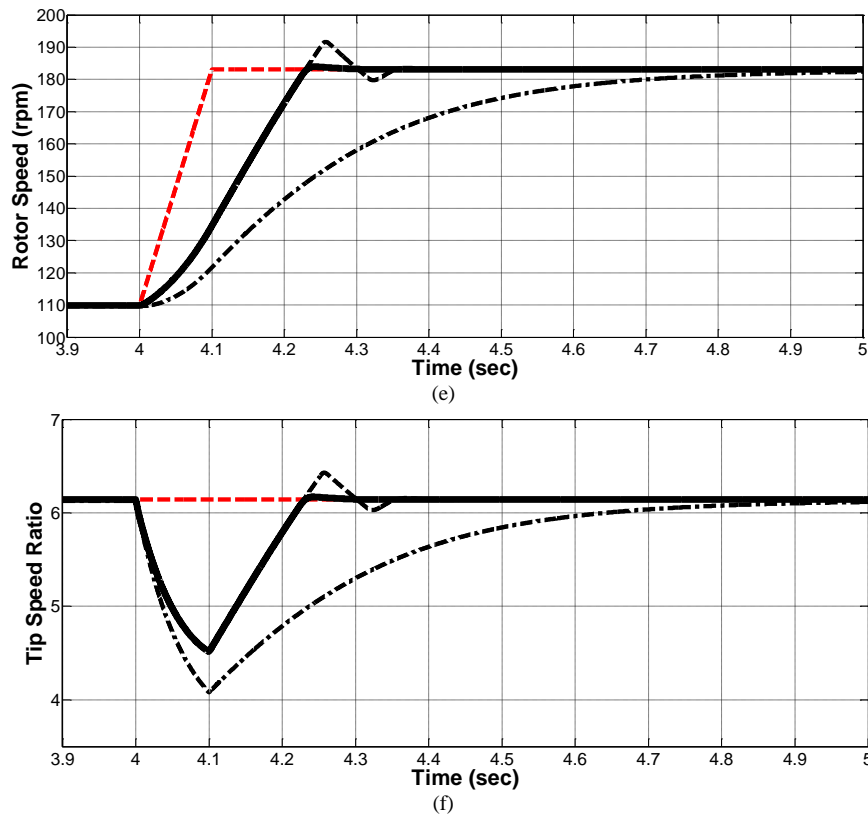


Fig (10): The transient and steady-state performance of WECS (a) applied wind speed (b) Rotational speed (c) Computed tip speed ratio (d) Power characteristics of WECS; maximum power curve of generator (solid), maximum power curve of turbine (dashed) and constant power curve (dashed-dotted) (e) comparison of rotational speed response via proposed FLC (solid), PI speed regulator (dashed) and directly applying $T_{m,opt}$ (dashed-dotted). (f) Comparison of tip speed ratio response via proposed FLC (solid), PI speed regulator (dashed) and directly applying $T_{m,opt}$ (dashed-dotted).

When the wind speed is below the rated wind speed $V_n = 12.5m/s$, the FLC tracks the applied step change very fast. Also the steady state operating points of system lies on MPPT curve (cf. OP1, OP2 and OP4 on Fig10(d)). Moreover the λ lies on $\lambda_{opt} = 6.15$. On the other hand, the torque limiting procedure should keep the operating point on the generator ratings at overrated wind speeds. This is verified by Fig. 10(d) for operating point corresponding to $t = 11.5$ s. It is obvious from Figs. 10(b) and 10(c) that the rotational speed is increased beyond the nominal value and the tip speed ratio is increased to decrease the harvested power from wind. It should be pointed out that the rated power of IPMSG not only is not a constant value, but also is dependent on rotational speed. Typically, the rated power at nominal rotational speed is considered as a criterion for power control at overrated wind speeds. Obviously from Fig. 10(d), our method harvests higher

power in comparison with the constant power method.

In order to prove superiority of our method, same wind profile is applied to WECSs equipped with the other two methods; a) directly applying $T_{m,opt}$ and b) PI speed regulator tuned manually. Figs. 7(e) and 7(f) compare the transient performance of three methods by zooming in on a time interval around the applied step changes at $t = 4$ s. The results show that our approach considerably improves the system response time.

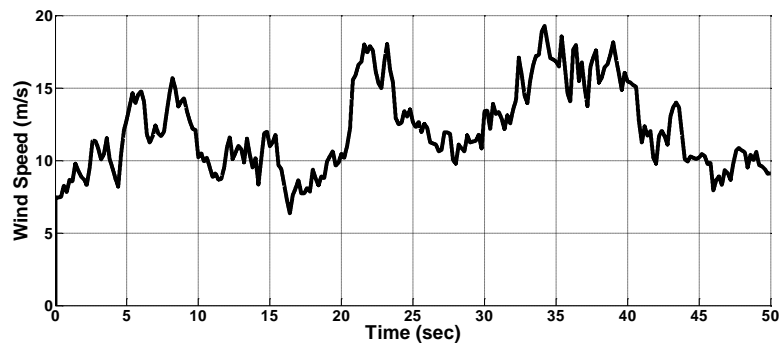
The performance of our proposed overall control strategy is evaluated in presence of actual wind variations. Fig. 11(a) shows an interval of measured wind variations applied to the WECS. The wind pattern is selected in such a way that enables us to evaluate the control scheme performance for a wide wind speed range. Fig. 11(b) shows the measured rotational speed (solid) together with desired rotational speed for MPPT (dashed) computed by (3). For

wind speed under 12.5 m/s, these two curves met each other, which verifies the effectiveness of proposed controller for MPPT operation. Moreover, it is obvious from Fig. 11(c) that the λ lies in a small neighborhood around the λ_{opt} . As the wind speed exceeds 12.5 m/s the MPPT is left and the harvested power is limited to the rated power of generator (cf. Fig 11(d)). Obviously, from Figs. 11(b) and 11(c), the rotational speed and tip speed ratio are increased during mentioned intervals to keep power ratings.

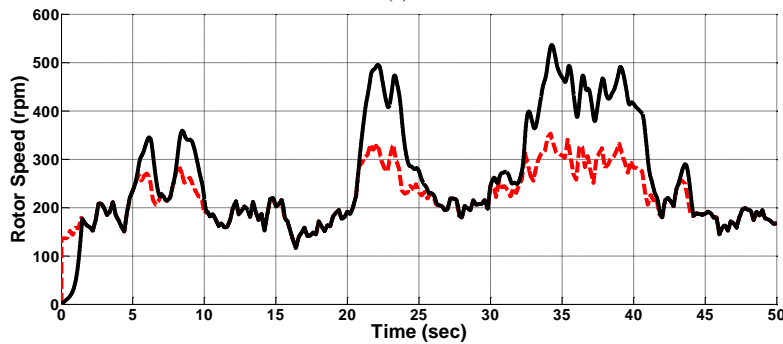
Concerning sharp power pulsation in harvested electrical power, we note that such sharp electrical power transients do not mean the mechanical power will have the same behavior due to inertia of the rotor. The difference between the electrical power and the mechanical one introduces the charging/discharging power

of the rotor inertia [35]. In particular, the difference charges (discharges) the rotor inertia when the electrical power is smaller (greater) than the mechanical one. Such charging (discharging) implies the acceleration (deceleration) of the rotor.

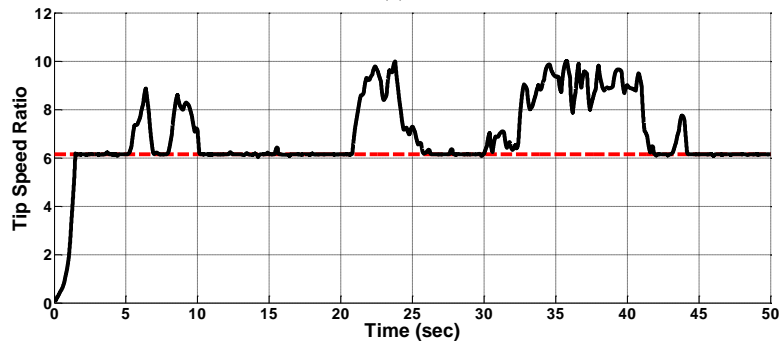
The estimated flux and its reference are illustrated in Fig. 11(e). As expected, the flux is weakened for operation over nominal rotational speed. Fig 11(f) shows the effective value of stator current. It is obvious that the current resides under the nominal value. This confirms the successful operation of the proposed control method. The difference between generated copper loss and nominal copper loss is presented in Fig. 11(g). Although the copper loss minimization is not performed at rated power generation, it is obvious during MPPT.



(a)



(b)



(c)

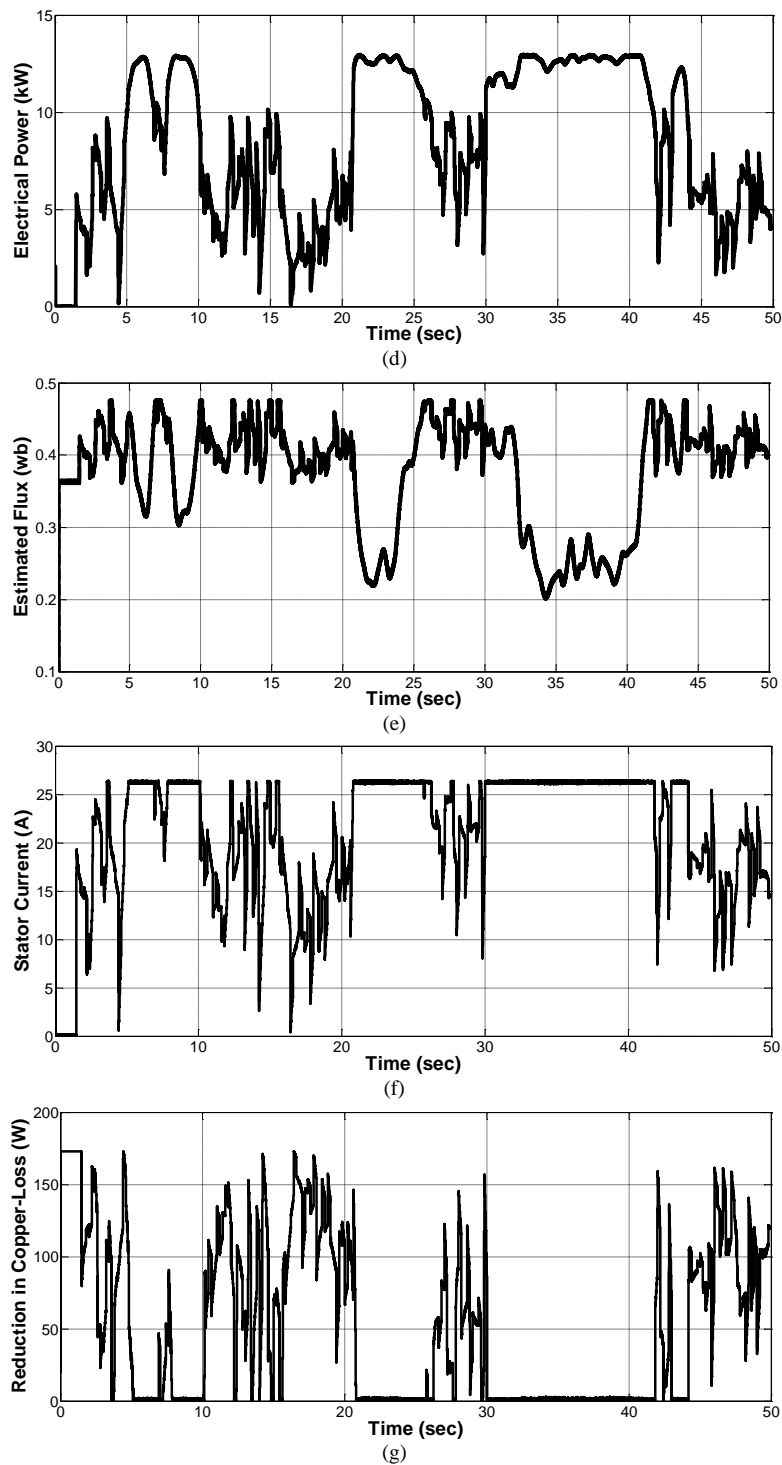


Fig (11): Performance of the proposed overall control strategy under a measured wind pattern (a) Applied wind pattern (b) Measured rotational speed (solid) and desired rotational speed forMPPT (dashed) (c) Computed tip speed ratio (solid) and optimal tip speed ratio (dashed) (d) Output power of WECS measured at DC-link (e) Estimated Flux magnitude (solid) and its reference (dashed) (f) effective value of stator current (g) reduction in copper loss compared with nominal copper loss

5. Conclusion

This paper presents an overall control strategy to control fixed-pitch small-scale WECS. The control scheme is actuated by a PWM converter allowing us to exploit the advantages of a SVM-DTC to control IPMSG. Compared to the existing related works, the MPPT operation is enhanced using a new FLC providing reference electrical torque. To avoid generator overload and retaining the operating point inside generator ratings at overrated wind speeds, the generated reference electrical torque of FLC has been limited. Also, the FLC is informed of the situation to prevent irrational growth of output. In this way, the system response is improved considerably. Moreover, the flux magnitude is provided using a lookup table in such a way that guarantees the machine operation over nominal speed, takes the machine limitations and minimizes the copper losses. It should be noted that the lookup table is derived by offline solving an optimization problem. Finally, the effectiveness of the proposed method has been verified under several scenarios.

References

- [1] REN21, "Renewables 2015 Global status report," 2015.
- [2] C. Bhende, S. Mishra, and S. G. Malla, "Permanent magnet synchronous generator-based standalone wind energy supply system," *IEEE Trans. Sustain. Energy* Vol. 2, pp. 361-373, 2011.
- [3] H. Li and Z. Chen, "Overview of different wind generator systems and their comparisons," *IET Renew. Power Gener.*, Vol. 2, pp. 123-138, 2008.
- [4] H. Chen, N. David, and D. Aliprantis, "Analysis of Permanent-Magnet Synchronous Generator With Vienna Rectifier for Wind Energy Conversion System," *IEEE Trans. Sustain. Energy* Vol. 4, pp. 154-163, 2013.
- [5] M. E. Haque, Y. Saw, and M. M. Chowdhury, "Advanced Control Scheme for an IPM Synchronous Generator-Based Gearless Variable Speed Wind Turbine," *IEEE Trans. Sustain. Energy* Vol. 5, pp. 354-362, 2014.
- [6] G. H. B. Foo, "Sensorless Direct Torque and flux control of interior permanent magnet synchronous motors at very low speeds including standstill," PhD thesis, University of New South Wales, 2010.
- [7] G.-D. Andreescu, C. I. Pitic, F. Blaabjerg, and I. Boldea, "Combined flux observer with signal injection enhancement for wide speed range sensorless direct torque control of IPMSM drives," *IEEE Trans. Energy Convers.*, Vol. 23, pp. 393-402, 2008.
- [8] N. Milivojevic, N. Schofield, I. Stamenkovic, and Y. Gurkaynak, "Field weakening control of PM generator used for small wind turbine application," in *Proc. IET Conf. Renewable Power Generation (RPG 2011)*, Edinburgh, Scotland, Sept. 2011, pp. 1-8.
- [9] Y. Inoue, S. Morimoto, and M. Sanada, "Control method for direct torque controlled PMSG in wind power generation system," in *Proc. IEEE Elect. Mach. Drives Conf. (IEMDC '09)*, Miami, USA, May 2009 pp. 1231-1238.
- [10] S. Morimoto, H. Nakayama, M. Sanada, and Y. Takeda, "Sensorless output maximization control for variable-speed wind generation system using IPMSG," *IEEE Trans. Ind. Appl.*, Vol. 41, pp. 60-67, 2005.
- [11] Z. Zhou, F. Sculler, J. F. Charpentier, M. El Hachemi Benbouzid, and T. Tang, "Power Control of a Nonpitchable PMSG-Based Marine Current Turbine at Overrated Current Speed With Flux-Weakening Strategy," *IEEE J. Ocean. Eng.*, Vol. 40, pp. 536 - 545 2014.
- [12] Z. M. Dalala, Z. U. Zahid, and J.-S. Lai, "New overall control strategy for small-scale WECS in MPPT and stall regions with mode transfer control," *IEEE Trans. Energy Convers.*, Vol. 28, pp. 1082-1092, 2013.
- [13] B. Neammanee, S. Sirisumranukul, and S. Chatratana, "Control Performance Analysis of Feedforward and Maximum Peak Power Tracking for Small-and Medium-Sized Fixed Pitch Wind Turbines," in *Proc. 9th Int. Conf. Control, Autom., Robot. Vision (ICARCV '06)*, Singapore, Dec. 2006, pp. 1-7.
- [14] J. Chen, J. Chen, and C. Gong, "New overall power control strategy for variable-speed fixed-pitch wind turbines within the whole wind velocity range," *IEEE Trans. Ind. Electron.*, Vol. 60, pp. 2652-2660, 2013.
- [15] A. Ahmed, L. Ran, and J. R. Bumby, "New constant electrical power soft-stalling control for small-scale VAWTs," *IEEE Trans. Energy Convers.*, Vol. 25, pp. 1152-1161, 2010.
- [16] Y. Zhao, C. Wei, Z. Zhang, and W. Qiao, "A review on position/speed sensorless control for permanent-magnet synchronous machine-based wind energy conversion systems," *IEEE J. Emerging Sel. Topics Power Electron.*, Vol. 1, pp. 203-216, 2013.
- [17] R. Cariveau, "Fundamental and Advanced Topics in Wind Power," Intech Publication, 2011.
- [18] V. Galdi, A. Piccolo, and P. Siano, "Designing an adaptive fuzzy controller for

- maximum wind energy extraction," *IEEE Trans. Energy Convers.*, Vol. 23, pp. 559-569, 2008.
- [19] Q. Zeng, L. Chang, and R. Shao, "Fuzzy-logic-based maximum power point tracking strategy for Pmsg variable-speed wind turbine generation systems," in *Electrical and Computer Engineering, 2008. CCECE 2008. Canadian Conference on, 2008*, pp. 000405-000410.
- [20] J. Yan, H. Lin, Y. Feng, X. Guo, Y. Huang, and Z. Zhu, "Improved sliding mode model reference adaptive system speed observer for fuzzy control of direct-drive permanent magnet synchronous generator wind power generation system," *IET Renew. Power Gener.*, Vol. 7, pp. 28-35, 2013.
- [21] G. Foo, S. Sayeef, and M. Rahman, "Low-speed and standstill operation of a sensorless direct torque and flux controlled IPM synchronous motor drive," *IEEE Trans. Energy Convers.*, Vol. 25, pp. 25-33, 2010.
- [22] E. Hau, "Rotor Aerodynamics," in *Wind Turbines Fundamentals, Technologies, Application, Economics*, E. Hau, Ed., ed: Springer, Berlin Heidelberg, 2013, pp. 89-166.
- [23] P. W. Carlin, A. S. Laxson, and E. Muljadi, "The history and state of the art of variable-speed wind turbine technology," *Wind Energy*, vol. 6, pp. 129-159, 2003.
- [24] M. T. Seitzler, "The Electrical and Mechanical Performance Evaluation of a Roof-mounted One Kilowatt Wind Turbine," University of California, Davis CWEC-2009-003, 2009.
- [25] M. Abarzadeh, H. M. Kojabadi, and L. Chang, "Small Scale Wind Energy Conversion Systems," in *Wind Turbines*, I. Al-Bahadly, Ed., ed Rimouski: InTech, Rimouski, 2011, pp. 639-652.
- [26] J. S. Thongam and M. Ouhrouche, "MPPT control methods in wind energy conversion systems," in *Fundamental and Advanced Topics in Wind Power*, R. Carriveau, Ed., ed: InTech, 2011, pp. 339-360.
- [27] T.-S. Zhan, J. L. Chen, S.-J. Chen, C.-H. Huang, and C.-H. Lin, "Design of a chaos synchronisation-based maximum power tracking controller for a wind-energy-conversion system," *IET Renew. Power Gener.*, Vol. 8, pp. 590-597, 2014.
- [28] B. Ramasamy, A. Palaniappan, and S. Yakoh, "Direct-drive low-speed wind energy conversion system incorporating axial-type permanent magnet generator and Z-source inverter with sensorless maximum power point tracking controller," *IET Renew. Power Gener.*, Vol. 7, pp. 284-295, 2013.
- [29] A. Miller, E. Muljadi, and D. S. Zinger, "A variable speed wind turbine power control," *IEEE Trans. Energy Convers.*, Vol. 12, pp. 181-186, 1997.
- [30] M. Morandini, E. Fornasiero, S. Bolognani, and N. Bianchi, "Torque and power rating of a wind-power PM generator drive for maximum profit-to-cost ratio," *IEEE Trans. Ind. Appl.*, Vol. 49, pp. 866-872, 2013.
- [31] P. Gill and E. Wong, "Sequential Quadratic Programming Methods," in *Mixed Integer Nonlinear Programming*. Vol. 154, J. Lee and S. Leyffer, Eds., ed: Springer, New York, 2012, pp. 147-224.
- [32] Z. Zhang, Y. Zhao, W. Qiao, and L. Qu, "A Discrete-Time Direct-Torque Control for Direct-Drive PMSG-Based Wind Energy Conversion Systems," *IEEE Trans. Ind. Appl.*, Vol. 51, pp. 3504 - 3514 2015.
- [33] Z. Zhang, Y. Zhao, W. Qiao, and L. Qu, "A Space-Vector-Modulated Sensorless Direct-Torque Control for Direct-Drive PMSG Wind Turbines," *IEEE Trans. Ind. Appl.*, Vol. 50, pp. 2331-2341, 2014.
- [34] D. Corbus and M. Meadors, "Small Wind Research Turbine Final Report," 2005.
- [35] Z. Qin, F. Blaabjerg, and P. C. Loh, "A Rotating Speed Controller Design Method for Power Leveling by Means of Inertia Energy in Wind Power Systems," *IEEE Trans. Energy Convers.*, Vol. 30, pp. 1052-1060, 2015.